Hindawi
Journal of Nanomaterials
Volume 2019, Article ID 5823969, 7 pages
https://doi.org/10.1155/2019/5823969

Research Article

Nanoscale Structures and Hydrogen Storage Capacity of Fe-C-H Produced by Milling Graphite with Steel Balls in a Hydrogen Atmosphere

Hiroaki Wakayama

Toyota Central R&D Laboratories, Inc., 41-1 Yokomichi, Nagakute, Aichi 480-1192, Japan

Correspondence should be addressed to Hiroaki Wakayama; wakayama@mosk.tytlabs.co.jp

Received 23 May 2019; Revised 22 August 2019; Accepted 27 August 2019; Published 9 September 2019

Academic Editor: Domenico Acierno

To elucidate the influence of Fe on the interaction between carbon and hydrogen in graphite nanocrystals, graphite nanocrystals were mechanically milled with steel balls in a hydrogen atmosphere, and the potential of the material produced to store hydrogen was evaluated. X-ray diffraction and Raman spectra revealed that milling reduced the graphene size and increased the average distance between graphene layers. Elemental analysis showed that milling increased both the H/C and Fe/C ratios in the material. After being milled in a hydrogen atmosphere, samples released hydrogen at a lower temperature than before milling. Thermal decomposition occurred in two stages—235 to 475°C and 692 to 749°C—and yielded a total of 1.0 wt% hydrogen. It is hypothesized that these two stages corresponded to hydrogen released from Fe_3C structures and from the Fe-catalyzed graphitization reaction, respectively. Before milling, samples slowly released a total of 0.5 wt% hydrogen over a temperature range from about 300 to over 900°C. Fe-C-H materials are attractive for hydrogen storage because they are composed of carbon and iron, which are inexpensive and abundant elements on Earth, and they have a high hydrogen weight density of 11 wt%.

1. Introduction

Nanocarbon materials such as carbon nanotubes, graphene, and fullerenes are often applied to lightweight structural materials [1, 2], heat dissipation materials [3, 4], and electrical conductors [5, 6] because they have high electrical and thermal conductivity. The expectation is that broader use of these nanocarbon materials in other applications will save energy. Of particular interest is their application to hydrogen storage materials [7–10].

The use of hydrogen as an energy source is being studied intensely; progress is being made in the development of various technologies such as fuel cell cars [11, 12], and attempts are underway to transform Iceland into a nation that relies primarily on hydrogen as a source of energy [13]. Hydrogen storage technology is important for hydrogen utilization technology. Hydrogen is currently stored in high-pressure cylinders [14], and improvement of storage efficiency is needed.

In recent years, there have been reports of highly efficient hydrogen storage (adsorption) in carbonaceous storage materials such as carbon nanotubes and graphite nanofibers. However, the characteristics of these methods (e.g., high release temperature) and problems with their insufficient practical properties and evaluation have precluded identification of a storage method that might be suitable for large-scale use in the future [15, 16]. The mechanism of hydrogen storage in carbonaceous materials is associated with the layered structure peculiar to graphite and may therefore differ from the mechanisms associated with other material systems.

Controlling the properties of nanocarbon materials requires control of the graphene layer structure. Heat treatment and vapor phase growth are examples of typical control

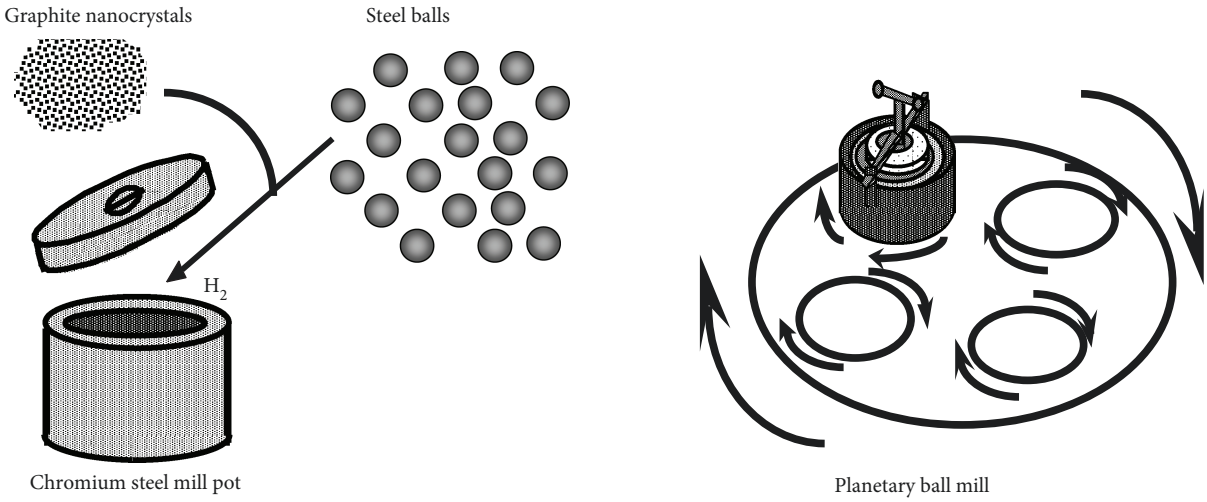

Figure 1: Schematic drawing of milling of graphite nanocrystals in a hydrogen atmosphere.

methods. Mechanical milling, which involves applying mechanical energy to materials and grinding them, does not require high temperatures; it is also possible to synthesize supersaturated alloys as well as amorphous or nonpermanent phase materials via mechanical milling. This process has attracted attention as a way to manufacture ceramic materials and alloys.

Mechanical milling of graphite with a ball mill in a hydrogen atmosphere has been reported to occlude a large amount of hydrogen in the solid phase [17]. The hydrogen storage capacity of this hydrogenated graphite is a unique property that results from milling, and the mechanism of storage is essentially different from that of typical hydrogen storage materials (e.g., $M+H_2 \Leftrightarrow MH_2$). The many studies of this mechanism reflect its potential as a means of storing hydrogen as well as its inherent interest as a subject of basic scientific research [17–20].

It has been suggested that iron, which is considered an impurity in the milling process, affects the interaction between carbon and hydrogen [21]. ESR measurements that recorded the unpaired electronic state (radical) in the sample revealed that localized electrons were generated as milling progressively destroyed the graphite structure [22].

In this study, the miniaturization of graphite nanocrystals was analyzed by Raman spectroscopy. Furthermore, the mechanism of hydrogen storage was inferred from the relationship between the graphite size and hydrogen storage capacity of milled samples. Graphite nanocrystals were mechanically milled with steel balls in a hydrogen atmosphere, and the nanostructural changes caused by mechanical milling were elucidated. Furthermore, the milled product was evaluated as a hydrogen storage material. The influence of Fe on the interaction between carbon and hydrogen was assessed. The mechanism of hydrogen release, in which Fe played an important role, was evaluated. Fe-C-H materials were found to be attractive for hydrogen storage because carbon and iron are inexpensive and abundant elements on Earth and because Fe-C-H materials have a high hydrogen weight density.

2. Materials and Methods

2.1. Sample Preparation

2.1.1. Preparation of Graphite Nanocrystals. Argon (99.99%) was introduced into a high-frequency induction thermal plasma generator (Denki Kogyo Co., Ltd.). Methane (99.99%) was then introduced into the Ar plasma for preparation of carbon samples. The internal pressure of the reaction vessel was 126 Torr, and the plate voltage was 5.5 kV. The flow rate of Ar as a plasma gas was 1.2 mL/min, and the flow rate of Ar as a sheath gas was 80 mL/min in the radial direction. The flow rate of CH_4 was 2 mL/min. Carbon samples attached to the inner wall of the reaction vessel were collected after the system had been operated for 60 min.

2.1.2. Milling of Graphite Nanocrystals in a Hydrogen Atmosphere. An aliquot of 0.5 g of graphite nanocrystals prepared as described in Section 2.1.1 was placed in a chromium steel mill pot (80 cc) together with 20 steel balls (10 mmϕ). Hydrogen gas was introduced at 1 MPa, and then, the system was operated as a planetary ball mill at 400 rpm for 80 h. Figure 1 shows a schematic diagram of the experimental apparatus.

2.2. Characterization. X-ray diffraction analysis, elemental analysis, laser Raman spectroscopy, and temperature-programmed desorption mass spectrometry (TPD-MS) measurements of samples prepared as described in Section 2.1 were carried out. X-ray diffraction (XRD) patterns were collected on a diffractometer (model RINT-TTR, Rigaku) (Cu Kα) operated at 40 kV and 50 mA. The d value was the spacing between the graphene layers, and L_a and L_c were the crystallite sizes along the a and c axes of the crystal, respectively. Elemental analysis for Fe and C was carried out by inductively coupled plasma-atomic emission spectrometry (ICP-AES; CIRIOS 120EOP, Rigaku). For quantitative analysis of hydrogen, a sample was placed in a graphite crucible and heated in an Ar stream to extract

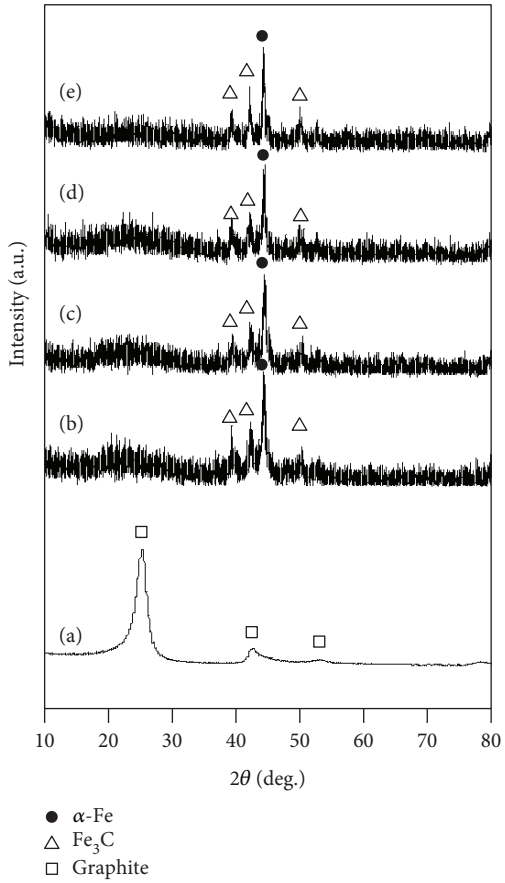

Figure 2: X-ray diffraction patterns of graphite nanocrystals (a) and samples milled in a hydrogen atmosphere for 10 (b), 20 (c), 40 (d), and 80 h (e).

Table 1: The average surface distance (d) calculated from the peak position of the (002) peak.

Milling time (h)	d (Å)
0	3.44
10	3.75
20	3.73
40	3.76
80	3.70

hydrogen as H_2, which was detected and quantified with a thermal conductivity detector (TCD).

Raman spectra of the mechanically ground samples were measured with a JASCO NR-1000S Raman spectrometer equipped with an Ar ion laser (GLG3300, NEC), a double monochromator (CT-1000, JASCO), and a photomultiplier (R464, Hamamatsu Photonics, K.K.). A 488 nm laser line with an output power of 300 mW was focused to a diameter of 80 mmϕ on the sample, and scattered light was collected at 30° to the incident laser beam. The spectrum resolution was about 10 cm^{-1}. The gas generated from the samples as the temperature varied from 30 to 1050°C at 10°C/min was analyzed with a TPD-MS (TPD: Ohkura ATD 700, MS: ANELVA AGS-221). The gases that evolved during the heating process were continuously and quantitatively analyzed with a mass spectrometer. Before the experiments, the mass spectrometer was calibrated using N_2, H_2, CO, CO_2, O_2, CH_4, and Ar. The total pressure of the gas released during the heat treatment was also measured as a function of temperature with a Bayard–Alpert gauge. The total gas pressure could then be compared to the pressure calculated from the

Table 2: Results of elemental analysis of graphite nanocrystals milled in a hydrogen atmosphere.

Milling time (h)	H/C (wt%)	Fe/C (wt%)
0	2.4	0.0
10	5.6	3.1
20	4.9	3.3
40	5.7	2.5
80	5.0	3.0

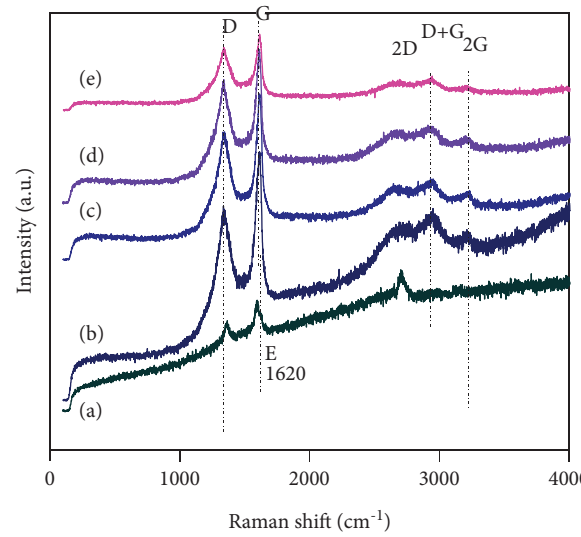

Figure 3: Laser Raman spectroscopy of graphite nanocrystals (a) and samples milled in a hydrogen atmosphere for 10 (b), 20 (c), 40 (d), and 80 h (e).

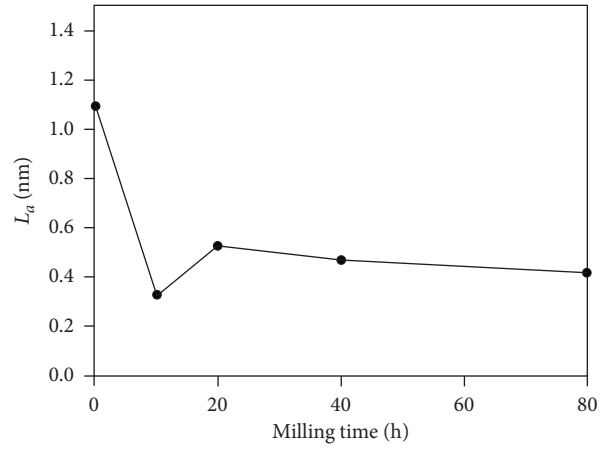

Figure 4: Crystallite size (L_a) of graphite nanocrystals milled in a hydrogen atmosphere.

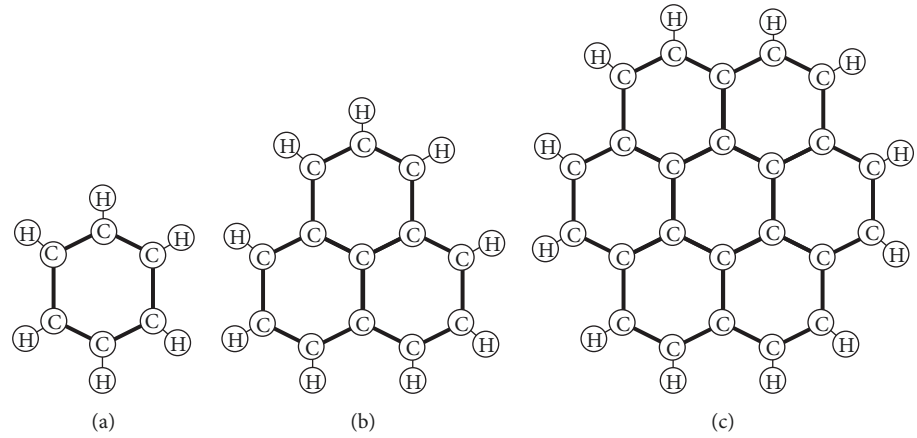

Figure 5: Structural formulae of benzene (a), phenalenyl (b), and coronene (c).

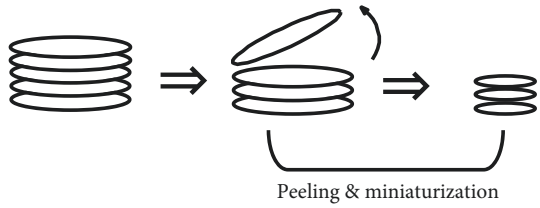

Figure 6: Mechanism of miniaturization of graphite nanocrystals.

sum of the partial pressures of the gas species deduced from the quantitative analysis of the gas phase. The desorption rate of each gas as a function of temperature was determined from the TPD analysis. The total amount of each gas released was computed by temporal integration of the TPD curves.

3. Results and Discussion

3.1. XRD. XRD graphite peaks of (002), (10), and (004) were found for graphite nanocrystals (Figure 2(a)). Regardless of the milling time, small (002) peaks at 20–30° derived from the order in the interlayer direction of the graphite (*c* axis direction) could be confirmed, and the α-Fe and Fe_3C peaks at 40–50° due to contamination from the steel balls could also be confirmed (Figure 2(b)–(e)). Table 1 shows the average surface distance (d) calculated from the position of the (002) peak. The d value of the milled samples was larger after milling. These results show that the milling process increased the interlayer distance in the graphite nanocrystals of the milled samples.

3.2. Elemental Analysis. Table 2 shows the results of the elemental analysis of graphite nanocrystals milled in a hydrogen atmosphere. In all cases, the H/C ratio was about 4.9–5.7 wt%. It was apparent that hydrogen was introduced by milling. The amount of introduced hydrogen was not very dependent on the milling time. Based on the changes in the values of d in Table 1, it is hypothesized that the layered structure of the graphite was destroyed by milling and that hydrogen was introduced at that time. The Fe/C ratio was about 2.5–3.3 wt%. It is inferred that Fe was an impurity introduced during the milling process.

3.3. Laser Raman Spectroscopy. The laser Raman spectroscopy peaks (G band peaks) derived from the graphite structures at around 1580 cm^{-1} and peaks (D band peaks) derived from disorder structures at around 1350 cm^{-1} were apparent in the spectra of all samples (Figure 3). The crystallite size (L_a) in the spreading direction of the hexagonal planes of the graphite structures (*a* to *b* axis direction) was calculated from the calibration equation of Tuinstra and Koenig [23]:

$$L_a = 4.2 \frac{A_G}{A_D}, \quad (1)$$

where A_G is the integrated intensity of the G band peak, and A_D is the integrated intensity of the D band peak. Regardless of the milling time, L_a values for all milled samples were about 0.5 nm (Figure 4).

Next, the atomic ratio of hydrogen to carbon in the aromatic structure was considered. Figure 5 shows the structural formulae of benzene, phenalenyl [24, 25], and coronene. The atomic ratios of hydrogen to carbon are 6/6, 9/13, and 12/24, respectively, in these molecules, and the corresponding weight percents of hydrogen are 8.33, 5.76, and 2.78 wt%. The weight percent of hydrogen for phenalenyl was close to the result in Table 2 for milled samples (4.9–5.7 wt%). The size of L_a for phenalenyl was 0.56 nm, which is almost the same as the result for all milled samples (approx. 0.5 nm). It is therefore assumed that the milled samples were graphene with a size similar to that of phenalenyl.

Figure 6 shows the mechanism of miniaturization of graphite nanocrystals. When milling in hydrogen, miniaturization was possible at a lower revolution number than in the case of milling in an inert atmosphere. It is hypothesized that the miniaturization process was accelerated because hydrogen was stabilized on the miniaturized edge carbon atoms, and the suppression of recombination and promotion of miniaturization were therefore enhanced.

The hydrogen absorption state of ball-milled carbon includes not only –CH but also $-CH_2$, $-CH_3$, or both. In IR and neutron-scattering experiments, it has been confirmed that hydrocarbon groups (–CH, $-CH_2$, and $-CH_3$)

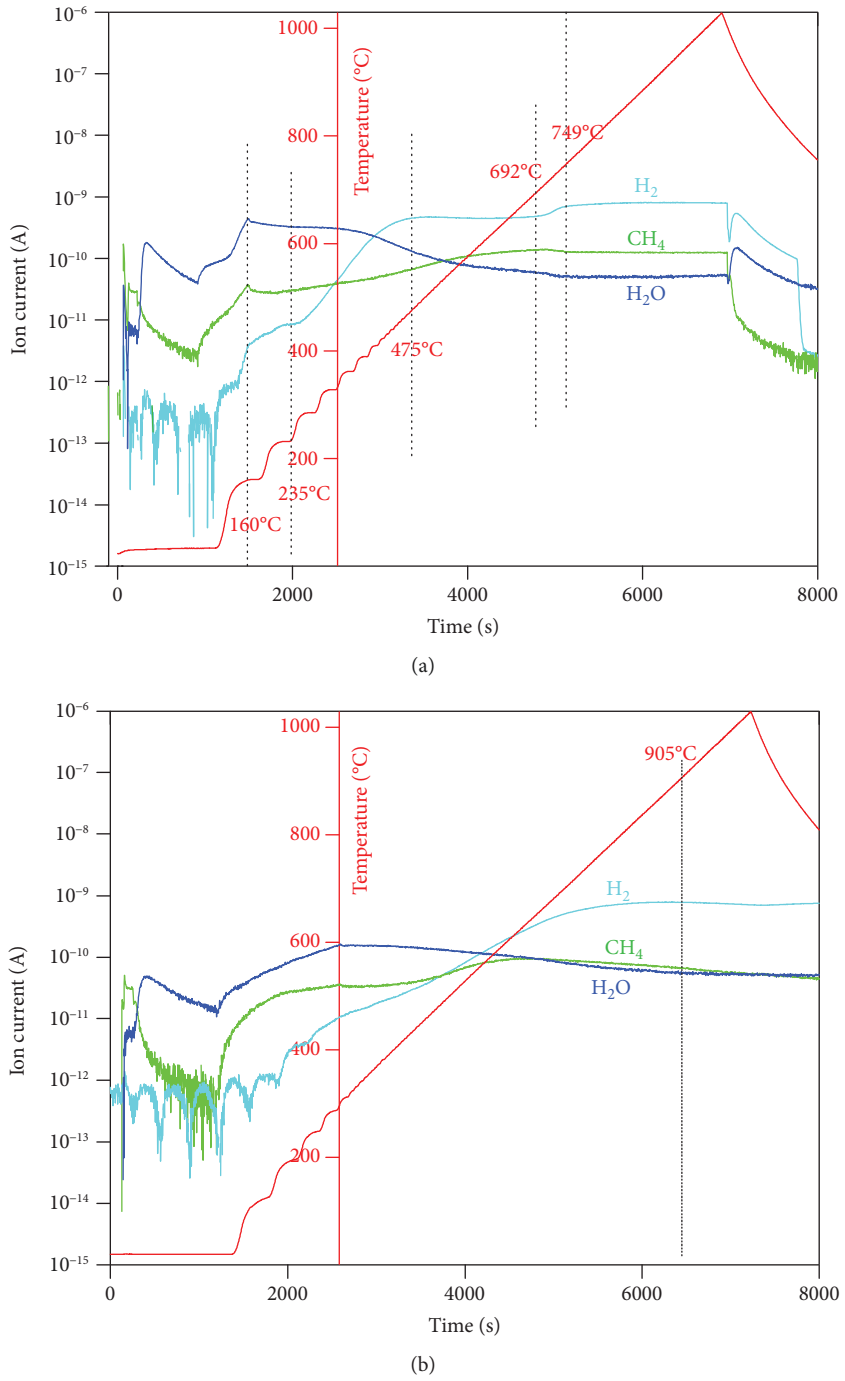

Figure 7: TPD-MS spectra of a graphitic microcrystal milled for 20 h in a hydrogen atmosphere (a) and of the sample before milling (b).

are generated by hydrogen storage [26, 27]. These results have shown that edges and defects with active electrons are generated in the process of destroying the graphite structures by milling and hydrogen bonds are formed at those sites. The correlation between the structural change and hydrogen content observed in this study is consistent with the hydrogenation mechanisms described in previous reports.

3.4. TPD-MS. Figure 7(a) shows the TPD-MS spectra of graphitic nanocrystals milled for 20 h in a hydrogen atmosphere. Figure 8 shows the temperature dependence of the amount of hydrogen released from the graphite nanocrystals before and after milling in a hydrogen atmosphere based on the TPD-MS results (Figure 7). The results show that the sample milled in a hydrogen atmosphere began to release hydrogen at a temperature of 300°C, lower than that of the sample before milling. In the milled graphite nanocrystals, 1.0 wt% of hydrogen was generated. Thermal decomposition occurred in two stages: 235–475°C and 692–749°C. The amount of hydrogen generated increased

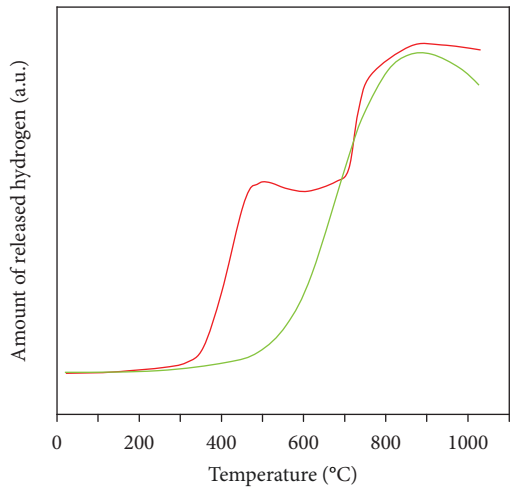

Figure 8: Temperature dependence of the amount of hydrogen released from a graphite microcrystal milled for 20 h in a hydrogen atmosphere (red curve) and graphite microcrystal before milling (green curve).

remarkably at 400°C or higher. In contrast, the sample before milling released hydrogen from about 300°C to over 900°C (Figure 7(b)). A total of 0.5 wt% of hydrogen was generated from the sample before milling.

High temperatures of several thousand °C are generally required to graphitize carbon-based materials, but it has been reported that graphitization proceeds at lower temperatures when Fe nanoparticles are used as catalysts [28]. Growth of the graphite crystal likely occurs on the Fe surface. Nanosized Fe is probably a result of Fe incorporation by milling and acts as a catalyst for graphitization.

Examination of the high-temperature region of the hydrogen release profile (Figure 8) revealed that hydrogen release proceeded slowly up to a temperature of 900°C or higher in the sample before milling, which did not contain Fe, whereas in the milled sample, hydrogen release was almost complete after the steep hydrogen release peak at 700°C.

This difference can be explained by considering the characteristics of the hydrogen storage states of the graphites. Hydrogen at C-H sites in the edges or defects of graphites can be thermally released by simple C-H bond breakage because of structural destruction caused by the milling process. Hydrogen release is considered to have a wide temperature distribution according to the energy distribution of hydrogen storage states. In contrast, in the case of a milled sample, graphitization proceeded at about 700°C because of the catalytic effect of Fe; the edges and defects that are hydrogen storage sites recombined during crystallization [28]. In this case, hydrogen was released rapidly from C-H sites. Finally, hydrogen trapped at the distorted interface between Fe and Fe_3C or at the disordered interface between lamellar structures of Fe_3C can be desorbed at about 400°C [29]. These experimental facts are very consistent with the results obtained in this study. Our results are therefore consistent with the hypothesis that hydrogen is stored in the disordered C-Fe phase and released at around 450°C during the structural change.

TPD-MS analyses of the milled sample indicate that 1.0 wt% hydrogen was released. If the 0.5 wt% obtained from a sample before milling is the hydrogen release capacity of a C-H site, then the hydrogen release capacity of a C-Fe-H site is 0.5 wt%. In the milled sample, the weight ratio of C and Fe was Fe/C = 3.3 wt%, so the weight ratios of C, Fe, and H in the milled sample were 96.3, 3.2, and 0.5 wt%, respectively. Assuming that a disordered C-Fe phase was formed at C : Fe = 1 : 1 (mol), the weight percentage of C in the C-Fe-H site was $(3.2/55.85)^{*}12.01 = 0.7$ wt%. Thus, the C-Fe-H site contained H/(C-Fe-H) equal to $0.5/(0.7 + 3.2 + 0.5) = 11$ wt %. The implication is that a large amount of hydrogen can be released from the C-Fe-H site in the milled material. This hydrogen weight density is much higher than that of alloy materials, which are conventional hydrogen storage materials, and is a value comparable to that of light-element hydrogen storage materials.

If a C-Fe phase can be selectively synthesized, it can function as a material with a high hydrogen storage capacity and can release hydrogen at about 450°C. The characteristics required for practical use imply that the hydrogen release temperature should be low. However, the C-Fe phase is an attractive material for hydrogen storage because it is composed of carbon and iron, which are inexpensive and abundant elements on Earth, and it has a high hydrogen weight density.

4. Summary

In order to elucidate the influence of Fe, which has been considered to be an impurity introduced during the milling process, on the interaction between carbon and hydrogen, graphite nanocrystals were mechanically milled with steel balls in a hydrogen atmosphere, and the nanostructural changes of carbon caused by mechanical milling are elucidated. Furthermore, the characteristics of Fe-C-H as a hydrogen storage material were evaluated. The hydrogen release mechanism, in which Fe plays an important role, was also evaluated. Fe-C-H materials were found to be attractive materials for hydrogen storage because they are composed of carbon and iron, which are inexpensive and abundant elements on Earth, and they have a high hydrogen weight density.

Data Availability

All the data used to support the findings of this study are available from the corresponding author upon request.

Conflicts of Interest

The author declares no competing financial interest.

References

[1] V. Singh, D. Joung, L. Zhai, S. Das, S. I. Khondaker, and S. Seal, "Graphene based materials: past, present and future," *Progress in Materials Science*, vol. 56, no. 8, pp. 1178–1271, 2011.

[2] V. N. Popov, "Carbon nanotubes: properties and application," *Materials Science and Engineering: R: Reports*, vol. 43, no. 3, pp. 61–102, 2004.

[3] E. Pop, V. Varshney, and A. K. Roy, "Thermal properties of graphene: fundamentals and applications," *MRS Bulletin*, vol. 37, no. 12, pp. 1273–1281, 2012.

[4] K. Kordás, G. Tóth, P. Moilanen et al., "Chip cooling with integrated carbon nanotube microfin architectures," *Applied Physics Letters*, vol. 90, no. 12, article 123105, 2007.

[5] N. Zhu, W. Liu, M. Xue et al., "Graphene as a conductive additive to enhance the high-rate capabilities of electrospun $Li_4Ti_5O_{12}$ for lithium-ion batteries," *Electrochimica Acta*, vol. 55, no. 20, pp. 5813–5818, 2010.

[6] B. J. Landi, M. J. Ganter, C. D. Cress, R. A. DiLeo, and R. P. Raffaelle, "Carbon nanotubes for lithium ion batteries," *Energy & Environmental Science*, vol. 2, no. 6, pp. 638–654, 2009.

[7] A. C. Dillon, K. M. Jones, T. A. Bekkedahl, C. H. Kiang, D. S. Bethune, and M. J. Heben, "Storage of hydrogen in single-walled carbon nanotubes," *Nature*, vol. 386, no. 6623, pp. 377–379, 1997.

[8] C. Liu, Y. Y. Fan, M. Liu, H. T. Cong, H. M. Cheng, and M. S. Dresselhaus, "Hydrogen storage in single-walled carbon nanotubes at room temperature," *Science*, vol. 286, no. 5442, pp. 1127–1129, 1999.

[9] A. Chambers, C. Park, R. T. K. Baker, and N. M. Rodriguez, "Hydrogen storage in graphite nanofibers," *The Journal of Physical Chemistry B*, vol. 102, no. 22, pp. 4253–4256, 1998.

[10] P. Chen, X. Wu, J. Lin, and K. L. Tan, "High H_2 uptake by alkali-doped carbon nanotubes under ambient pressure and moderate temperatures," *Science*, vol. 285, no. 5424, pp. 91–93, 1999.

[11] D. K. Ross, "Hydrogen storage: the major technological barrier to the development of hydrogen fuel cell cars," *Vacuum*, vol. 80, no. 10, pp. 1084–1089, 2006.

[12] T. Wilberforce, Z. el-Hassan, F. N. Khatib et al., "Developments of electric cars and fuel cell hydrogen electric cars," *International Journal of Hydrogen Energy*, vol. 42, no. 40, pp. 25695–25734, 2017.

[13] S. Park, "Iceland's hydrogen energy policy development (1998–2007) from a sociotechnical experiment viewpoint," *International Journal of Hydrogen Energy*, vol. 36, no. 17, pp. 10443–10454, 2011.

[14] L. Wang, C. Zheng, S. Wei, B. Wang, and Z. Wei, "Thermo-mechanical investigation of composite high-pressure hydrogen storage cylinder during fast filling," *International Journal of Hydrogen Energy*, vol. 40, no. 21, pp. 6853–6859, 2015.

[15] C. C. Ahn, Y. Ye, B. V. Ratnakumar, C. Witham, R. C. Bowman Jr., and B. Fultz, "Hydrogen desorption and adsorption measurements on graphite nanofibers," *Applied Physics Letters*, vol. 73, no. 23, pp. 3378–3380, 1998.

[16] R. T. Yang, "Hydrogen storage by alkali-doped carbon nanotubes–revisited," *Carbon*, vol. 38, no. 4, pp. 623–626, 2000.

[17] H. Imamura, M. Kusuhara, S. Minami et al., "Carbon nanocomposites synthesized by high-energy mechanical milling of graphite and magnesium for hydrogen storage," *Acta Materialia*, vol. 51, no. 20, pp. 6407–6414, 2003.

[18] F. Liu, X. Zhang, J. Cheng et al., "Preparation of short carbon nanotubes by mechanical ball milling and their hydrogen adsorption behavior," *Carbon*, vol. 41, no. 13, pp. 2527–2532, 2003.

[19] T. Ichikawa, D. M. Chen, S. Isobe, E. Gomibuchi, and H. Fujii, "Hydrogen storage properties on mechanically milled graphite," *Materials Science and Engineering: B*, vol. 108, no. 1-2, pp. 138–142, 2004.

[20] Z. Huang, A. Calka, and H. Liu, "Effects of milling conditions on hydrogen storage properties of graphite," *Journal of Materials Science*, vol. 42, no. 14, pp. 5437–5441, 2007.

[21] H. Miyaoka, T. Ichikawa, T. Fujii et al., "Anomalous hydrogen absorption on non-stoichiometric iron-carbon compound," *Journal of Alloys and Compounds*, vol. 507, no. 2, pp. 547–550, 2010.

[22] C. I. Smith, H. Miyaoka, T. Ichikawa et al., "Electron spin resonance investigation of hydrogen absorption in ball-milled graphite," *Journal of Physical Chemistry C*, vol. 113, no. 14, pp. 5409–5416, 2009.

[23] F. Tuinstra and J. L. Koenig, "Raman spectrum of graphite," *The Journal of Chemical Physics*, vol. 53, no. 3, pp. 1126–1130, 1970.

[24] D. H. Reid, "The chemistry of the phenalenes," *Quarterly Reviews, Chemical Society*, vol. 19, no. 3, pp. 274–302, 1965.

[25] R. Pettit, "The synthesis and properties of the perinapthenylium cation," *Journal of the American Chemical Society*, vol. 82, no. 8, pp. 1972–1975, 1960.

[26] K. Itoh, Y. Miyahara, S. I. Orimo, H. Fujii, T. Kamiyama, and T. Fukunaga, "The local structure of hydrogen storage nanocrystalline graphite by neutron scattering," *Journal of Alloys and Compounds*, vol. 356-357, pp. 608–611, 2003.

[27] N. Ogita, K. Yamamoto, C. Hayashi et al., "Raman scattering and infrared absorption investigation of hydrogen configuration state in mechanically milled graphite under H_2 gas atmosphere," *Journal of the Physical Society of Japan*, vol. 73, no. 3, pp. 553–555, 2004.

[28] L. Wan-Qiang, M. Hong-An, L. Xiao-Lei et al., "Effect of carbon source with different graphitization degrees on the synthesis of diamond," *Chinese Physics Letters*, vol. 24, no. 6, pp. 1749–1752, 2007.

[29] D. G. Enos and J. R. Scully, "A critical-strain criterion for hydrogen embrittlement of cold-drawn, ultrafine pearlitic steel," *Metallurgical and Materials Transactions A: Physical Metallurgy and Materials Science*, vol. 33, no. 4, pp. 1151–1166, 2002.